Finite temperature spectral functions of the linear $O(N)$-model at large N applied to the $\pi - \sigma$ system

A. Patkós[a*], Zs. Szép[a†] and P. Szépfalusy[a,b‡]
[a]Eötvös University, H-1117 Budapest, Hungary
[b] Research Institute for Solid State Physics and Optics, H-1525, Budapest, Hungary

October 28, 2018

Abstract

The thermal evolution of the spectral densities derivable from the two-point functions of the elementary and the quadratic composite fields of the $O(N)$ model is studied in the isosinglet channel and in the broken symmetry phase at infinite N. The results are applied with realistic parameter values to the $N = 4$ case. They provide a reasonable description of the σ meson at $T = 0$. Threshold enhancement is observed around $T \sim 1.07 m_\pi$. For higher temperatures the maximum of the spectral function in the single meson channel decreases and becomes increasingly rounded.

1 Introduction

There is increasing interest in finding signatures for the characterisation of strongly interacting matter around the transition temperature from the hadronic to the quark-gluon regime. Density and temperature induced features of the correlations in the soft pion spectra is a frequently discussed issue. The majority of these pions comes from resonance decay. One expects that temperature induced shifts in the position and width of the ρ and σ pole location is sensitively reflected in the spectra.

The effects related to the variation of the location and the width of the broad σ resonance were investigated in the past decade systematically [1]. The main theoretical framework of these investigations was the $O(4)$ linear sigma-model. Various reorganisations of the perturbative series [2] were proposed for the self-energy calculations. Despite of the rather large value of the nonlinear coupling $\lambda_R \approx \mathcal{O}(30 - 70)$, one loop calculations gave important qualitative hints for the enhancement of the spectral function in

*Dept. of Atomic Physics, e-mail: patkos@ludens.elte.hu
†Dept. of Atomic Physics, e-mail: szepzs@cleopatra.elte.hu
‡Dept. of Physics of Complex Systems, e-mail: psz@complex.elte.hu

the σ-channel near the two-pion threshold as the temperature approaches the transition region.

In the non-relativistic context it has been recognised long time ago that in scalar theories the hybridisation [3] of the two-point functions of the elementary and quadratic composite fields play essential role in the determination of the elementary excitations in the whole temperature interval of the broken symmetry phase. Neutron scattering data on superfluid helium were successfully interpreted by taking into account the hybridisation[4].

Large N techniques are known to account for this phenomenon correctly, while ordinary perturbative approaches usually miss it [3, 5].

An additional point in favour of the use of the large N expansion is that it leads to a second order transition point in agreement with the well-known behaviour of the $O(N)$ model[6]. The lowest order computations done with any (even optimised) version of the conventional perturbation theory yield a first order phase transition when the temperature is increased.

Large N techniques are extensively studied also in connection with the out-of-equilibrium evolution and thermalisation of relativistic Bose-condensates [7, 8, 9, 10, 11], though the hybridisation in this respect did not receive till now much attention.

Our main goal with this investigation was to apply large N techniques for finding the finite temperature variation of the spectral function in the elementary and quadratic composite isosinglet channels, which influences the $\pi - \pi$ correlations measured in heavy ion collisions to a large extent. For this purpose the parametrisation of the linear $O(4)$-symmetric meson model is chosen to reproduce as closely as possible the accepted zero temperature fit to the complex mass, $M_\sigma - i\Gamma/2$ of this broad resonance [12].

In this Letter, after summarising the general formalism, mostly the results of the chirally invariant limiting case will be discussed, where the pions are massless, since the main ideas can be presented in this case very transparently. Results relevant for the case with explicit symmetry breaking will be presented shortly in the concluding part of the paper.

We shall work in the leading order large N approximation to the Schwinger-Dyson equations of the $O(4)$ model in the broken symmetry phase. The effect of next-to-leading order corrections is the subject of our ongoing research.

2 The model and its renormalised dynamical equations

The Lagrangian density including a term reflecting explicit breaking of the $O(N)$ symmetry is the following:

$$L = \frac{1}{2}[\partial_\mu \phi^a \partial^\mu \phi^a - m^2 \phi^a \phi^a] - \frac{\lambda}{24N}(\phi^a)^2(\phi^b)^2 + \sqrt{N} h \phi^1. \tag{1}$$

The broken symmetry phase can be studied after an appropriate shift, by introducing the symmetry breaking background:

$$\phi^a \to (\sqrt{N}\Phi + \phi^1, \phi^i). \tag{2}$$

The quantum field representing the fluctuations of the order parameter is termed σ, while the modes transversal to it are the Goldstone pions.

The equation of state, which determines the absolute value of the condensate comes from the requirement of the vanishing quantum expectation for the coefficient of the term linear in ϕ^1 in the shifted Lagrangian:

$$\langle\frac{\delta L}{\delta\phi^1}\rangle = 0 = \sqrt{N}\Phi\Big[m^2 + \frac{\lambda}{6}\Phi^2 + \frac{\lambda}{6N}\langle(\phi^a)^2\rangle - \frac{h}{\Phi}\Big]. \tag{3}$$

The quadratic fluctuations of the shifted fields are computed with an accuracy $\mathcal{O}(N^1)$, therefore only the contribution of the pions is retained. Anticipating a non-zero Goldstone mass due to the explicit symmetry breaking (which will be verified below) one finds the following relation connecting renormalised quantities (only contributions proportional to N^0 are kept):

$$m_R^2 + \frac{\lambda_R}{6}\Phi(T)^2 + \frac{\lambda_R}{96\pi^2}m_G^2(T)\ln\frac{m_G^2(T)e}{M_0^2} + \frac{\lambda_R T^2}{12\pi^2}\int_{\frac{m_G(T)}{T}}^{\infty} dy\frac{\sqrt{y^2 - \frac{m_G^2(T)}{T^2}}}{e^y - 1} = \frac{h}{\Phi(T)}. \tag{4}$$

Here the following renormalised couplings were introduced (momentum cut-off was applied for the regularisation of some divergent integrals):

$$\frac{m^2}{\lambda} + \frac{\Lambda^2}{96\pi^2} - \frac{m_R^2}{96\pi^2}\ln\frac{e\Lambda^2}{M_0^2} = \frac{m_R^2}{\lambda_R}, \qquad \frac{1}{\lambda} + \frac{1}{96\pi^2}\ln\frac{e\Lambda^2}{M_0^2} = \frac{1}{\lambda_R}. \tag{5}$$

The issue of the normalisation point M_0 will be discussed below.

At leading order ($N = \infty$) the only contribution to the self-energy of the Goldstone modes comes from the tadpole diagram. Therefore one has:

$$G_G^{-1}(p) = p^2 - m^2 - \frac{\lambda}{6}\Phi^2(T) - \frac{\lambda}{6N}\langle(\phi^a)^2\rangle = p^2 - \frac{h}{\Phi(T)}. \tag{6}$$

Here the sum representing the mass term was simplified in view of the equation of state (3). This equation implies that at $N = \infty$ the Goldstone particle is stable and its mass, $m_G^2(T) = h/\Phi(T)$ increases with the temperature.

With this identification the renormalised equation of state (4) can be cast into a more practical form by eliminating m_R^2 and h in favour of the $T = 0$ value of the condensate (Φ_0) and of the pion mass (m_{G0}):

$$\begin{aligned}&\frac{\lambda_R}{6}\frac{\Phi_0^2}{m_{G0}^2}\left(\frac{m_{G0}^4}{m_G^4} - 1\right) + \frac{\lambda_R}{96\pi^2}\left[\left(\frac{m_G^2}{m_{G0}^2} - 1\right)\ln\frac{m_{G0}^2 e}{M_0^2} + \frac{m_G^2}{m_{G0}^2}\ln\frac{m_G^2}{m_{G0}^2}\right]\\ +\quad &\frac{\lambda_R T^2}{12\pi m_{G0}^2}\int_{m_G/T}^{\infty} dy\sqrt{y^2 - m_G^2/T^2}(e^y - 1)^{-1} = \frac{m_G^2}{m_{G0}^2} - 1.\end{aligned} \tag{7}$$

This form makes it clear that after λ_R and M_0/m_{G0} are chosen in the process of renormalisation at $T = 0$, one finds from this equation $m_G(T)/m_{G0}$ as a function of T/m_{G0} if the physical input $\Phi_0^3/h \equiv f_\pi^2/Nm_\pi^2$ is made.

The σ propagator receives $\mathcal{O}(N^0)$ contribution from the infinite iteration of the bubble diagrams $b(p)$, where on both lines Goldstone fields are propagating:

$$G_H^{-1}(p) = p^2 - \frac{h}{\Phi(T)} - \frac{\lambda}{3}\Phi^2(T)\frac{1}{1 - \lambda b(p)/6}. \tag{8}$$

Without entering its derivation we give here also the expression for the leading large N propagator of the quadratic composite field $(\phi^a\phi^a - \langle(\phi^a)^2\rangle)(\mathbf{x},t)$:

$$F(p) = \frac{(p^2 - h/\Phi(T))b(p)/6 + \Phi^2(T)/3}{(p^2 - h/\Phi(T))(1-\lambda_R b(p)/6) - \lambda_R\Phi^2(T)/3}. \tag{9}$$

It has the same denominator as $G_H(p)$ making explicit the hybridisation of the two objects.

The bubble contribution with external momentum $p_0, \mathbf{p}$ is the sum of a zero temperature and a T-dependent part, $b(p) = b_0(p) + b_T(p_0,\mathbf{p})$, which read as follows:

$$b_0(p) = \frac{1}{16\pi^2}\Big(-\ln\frac{e\Lambda^2}{M_0^2} + \ln\frac{m_G^2}{M_0^2} - \sqrt{1-4m_G^2/p^2}\ln\frac{\sqrt{1-4m_G^2/p^2}-1}{\sqrt{1-4m_G^2/p^2}+1}\Big), \tag{10}$$

$$\begin{aligned} b_T(p) \;=\; & \int\frac{d^3\mathbf{q}}{(2\pi)^3}\frac{1}{4\omega_1\omega_2}\left\{(n_1+n_2)\left[\frac{1}{p_0-\omega_1-\omega_2+i\epsilon} - \frac{1}{p_0+\omega_1+\omega_2+i\epsilon}\right]\right. \\ & \left. -(n_1-n_2)\left[\frac{1}{p_0-\omega_1+\omega_2+i\epsilon} - \frac{1}{p_0+\omega_1-\omega_2+i\epsilon}\right]\right\}, \end{aligned} \tag{11}$$

where $n_i = 1/(\exp(\beta\omega_i)-1)$ and $\omega_1 = (\mathbf{q}^2+m_G^2)^{1/2}, \omega_2 = ((\mathbf{q}+\mathbf{p})^2+m_G^2)^{1/2}$. The first term in the expression of $b_0(p)$ is cancelled in the expression of the σ propagator by the divergence of the bare coupling λ and the inverse propagator, expressed in terms of the renormalised quantities is finite. Note, that $b_0(p)$ has to be evaluated with $m_G(T)$!

The phenomenologically most interesting object is the spectral function of the order parameter field σ, defined as

$$\rho_H(p_0,\mathbf{p},T) = -\frac{1}{\pi}\mathrm{Im}G_H(p_0,\mathbf{p},T). \tag{12}$$

For non-zero T ρ_H has a singularity at $p_0 = 0$ due to the Bose-Einstein factor $n(\beta p_0/2)$. In the chiral limit $h = 0$ this point coincides with the two-pion threshold. In order to make the effects related to the physical excitations visible around this point in Fig.1 we show $\rho_1(p_0,0,T)T_c^2 \equiv (1-\exp(-p_0/2T))\rho_H(p_0,0,T)T_c^2$. The curves are drawn for various temperatures below T_c and a representative value of $\lambda_R = 310$.

The temperature dependence of the order parameter needed for its evaluation is obtained from the equation of state which simplifies in this case [6] to

$$\frac{\Phi^2(T)}{T_c^2} = \frac{1}{12}\Big(1-\frac{T^2}{T_c^2}\Big), \qquad T_c^2 = 12\Phi_0^2. \tag{13}$$

The shape of the spectral density starts with a broad bump at $T = 0$ which is shifted towards lower frequencies when the temperature is increased. Already for $T = 0$ ρ_H has finite value at $p_0 = 0$, where its value is gradually increasing. At a temperature $T \sim 0.7T_c$ the bumpy structure at finite p_0 completely disappears and a simple Lorentzian shape develops with its maximum located at the threshold.

This evolution can be transparently interpreted if the temperature dependent location of the physical pole of the σ propagator is found. The physical pole is located in the lower half of the complex p_0-plane, therefore one is faced with the analytical continuation of $b_T(p)$ into the lower p_0-halfplane, since originally it is defined only in the upper halfplane by the Landau-prescription: $\epsilon > 0$. As becomes clear, this threshold enhancement is the manifestation of the gradual chiral symmetry restoration as T tends to T_c.

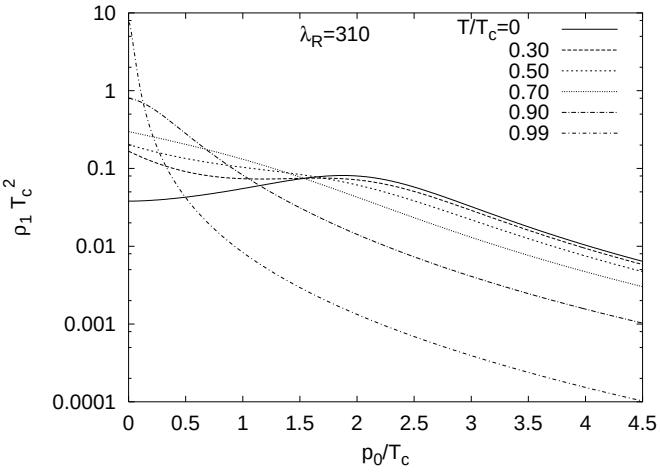

Figure 1: Temperature dependence of the modified spectral function ρ_1 in the σ meson channel for $h = 0$

3 The physical quasiparticle excitation in the σ channel

Below we give some details concerning the temperature variation of the excitation spectra and the interpretation of the spectral function with its help in the chiral limit ($h = 0$). One starts with the analysis at $T = 0$, where one fixes the renormalised parameters m_R^2, λ_R, remaining after h was set to zero. The renormalised mass is related to the size of the condensate (or in view of (13) to T_c) by the well-known equation: $-m_R^2/\Phi_0^2 = \lambda_R/6$.

λ_R will be chosen from a range where one finds for Γ/M_σ values which are the closest to the experimental one. For this we determine the $T = 0$ pole of the σ propagator by looking for the zeros of G_H^{-1} in terms of renormalised quantities:

$$G_H^{-1}(p) = p^2 - \frac{\lambda_R}{3}\Phi_0^2 \frac{1}{1 - \lambda_R \ln(-p^2/M_0^2)/96\pi^2} = 0. \tag{14}$$

The physical solution at rest of this equation is parametrised by putting $\mathbf{p} = 0, p_0 = M_0 \exp(-i\varphi_0), \pi/2 > \varphi_0 > 0$. (One can find its mirror solution in the third quarter). The notation shows, that the absolute value of the pole is chosen for the normalisation point defined in (5) and used in (10). If a physically satisfactory solution is found for some value λ_R with this normalisation point, the renormalisation group invariance of (14) ensures that for a different choice of M_0 the same ratio Γ/M_σ is found at some appropriately shifted value of λ_R. In this way the actual value of λ_R cannot be said to be large or small!

Since in view of (4) in the chiral limit one has a very simple equation for the critical temperature, our solution provides the mass $M_\sigma = M_0 \cos\varphi_0$ and the imaginary part $M_0 \sin\varphi_0$ in proportion of the critical temperature. It is interesting to note that using for $\sqrt{N}\Phi = 2\Phi$ the experimental value of f_π, eq.(13) gives $T_c = 161$ MeV, while the lattice simulations yield (173 ± 8) MeV [13]. The agreement is much better than expected. The real and imaginary parts of the complex physical pole are shown in Fig.2 as a function of λ_R.

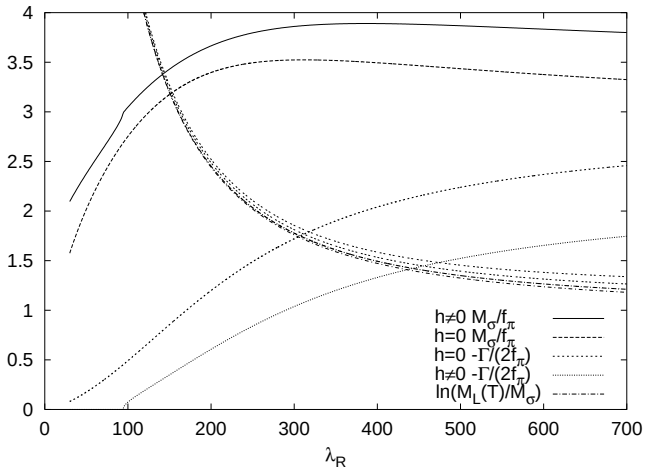

Figure 2: The imaginary and real parts of the physical poles at $T = 0$ in the chiral limit and also for $h \neq 0$. Also shown is the logarithm of the tachyon pole position in proportion to the mass of σ for various temperatures below T_c and for $h = 0$

In addition to the physical zeros of the inverse propagator scalar theories are known to have a tachyonic zero on the positive imaginary axis ($p_0 = iM_L$) (see [8] and references therein), which makes the theory unstable. Therefore the theory can be used as an effective theory until the physical scale M_0 is acceptably smaller than M_L. The position of the tachyonic zero is also found from (14). (The fact that the tachyonic pole shows up also in G_H not only in F is a manifestation of hybridisation). It is clear from Fig.2 that for $\lambda_R \leq 400$ one has $M_L/M_0 > 4$ and the effective approach is well justified. The representative value $\lambda_R = 310$ corresponds to a ratio $M_\sigma/\Gamma = 1$ at $T = 0$. The value of M_σ is estimated to be $7\Phi_0 \sim 350$ MeV.

At finite temperature we are interested in the temperature dependence of the σ-pole at rest, therefore we set $\mathbf{p} = 0$ in (11). The analytic continuation onto the lower plane can be carried out by adding to the expression of b_T valid in the upper halfplane a term which makes its imaginary part continuous when one approaches the real p_0-axis either from the upper or the lower halfplane:

$$\begin{aligned} b_T^{>}(p_0) &= \frac{1}{8\pi^2}\int_0^\infty dx \frac{1}{e^x-1}\Big[\frac{1}{z-x}-\frac{1}{z+x}\Big], \qquad z=\frac{p_0}{2T}, \qquad \text{Im } p_0 > 0, \\ b_T^{<}(p_0) &= b_T^{>}(p_0) - \frac{i}{4\pi}\frac{1}{\exp(z)-1}, \qquad \text{Im } p_0 < 0, \qquad \text{Re } p_0 > 0. \end{aligned} \tag{15}$$

The roots are parametrised the same way as in the $T = 0$ case, $p_0 = M(T)\exp(-i\varphi)$. After one determines $\Phi(T)$ from Eq.(13), from the complex equation

$$\begin{aligned} & 1 - \frac{\lambda_R}{96\pi^2}\Big(\ln\frac{M^2(T)}{M_0^2} - i(2\varphi+\pi)\Big) - \frac{\lambda_R}{3}\frac{\Phi^2(T)}{M^2(T)}e^{2i\varphi} - \frac{\lambda_R}{6}b_T^{>}(p_0 = Me^{-i\varphi}) \\ + \;& i\frac{\lambda_R}{24\pi}\frac{1}{\exp(M\exp(-i\varphi)/2T)-1} = 0 \end{aligned} \tag{16}$$

one can find the complex pole as a function of the temperature. All quantities are measured in units of $T_c \sim \Phi_0$.

Also at finite temperature one can study the tachyon solution in the upper halfplane using $b_T^>(iM_L)$. One might wonder if the temperature dependence of the tachyonic pole does not restrict further the coupling range where the effective use of the scalar theory is consistent. The broadening in Fig.2 of the line corresponding to the tachyonic pole reflects the slight decrease of its mass scale with increasing temperature. However, it is clear that in the region $\lambda_R < 400$, where the effective approach is consistent for $T = 0$, the position of the tachyon pole is practically unchanged.

Similarly, one can look directly for physical roots along the negative imaginary axis. Then using $b_T^<$ from (15) one finds that above a well-defined $T_{imag}(\lambda_R) < T_c$ the physical pole becomes purely imaginary: $-iM(T)$. If $\mu \equiv M(T)/2T << 1$, for the highest occupied low frequency region, one can use the expansion of the Bose-Einstein factors appearing in the last two terms of (16) with respect to the powers of μ and keep the leading terms:

$$1 - \frac{\lambda_R}{48\pi^2} \ln \frac{2T\mu}{M_0} + \frac{\lambda_R}{3} \frac{\Phi^2(T)}{4T^2} \frac{1}{\mu^2} - \frac{\lambda_R}{48\pi} \frac{1}{\mu} = 0. \tag{17}$$

This equation could have been derived directly, if one would have applied from the beginning the same approximation in Eq.(11). Clearly, the region around the origin (the critical region) can be analysed also directly with help of this simpler equation. Note that one has to go one step beyond the classical approximation to achieve a consistent approach.

The general pattern of the trajectory of the physical pole with increasing temperature was the following. The real part of its position started to diminish when T was raised. In this way the broad bump of the spectral function moves towards the origin, and its width is increasing due to the slight increase of its imaginary part. Depending on λ_R the root reaches at some $T_{imag} < T_c$ the negative imaginary axis and collides with its mirror root arriving from the third quarter. Each one is joining smoothly the trajectory of one of the pair of imaginary roots which appear just at T_{imag} and move opposite directions. We observe that the σ-bump gets lost in the background before the temperature reaches T_{imag}. The root approaching the origin along the imaginary axis produces in the spectral function a shrinking shape which becomes a Lorentzian only very close to T_c. Eventually for $T = T_c$ it builds up a term proportional to $\delta(p_0)/p_0$.

We see that the complex pole of the σ-propagator qualitatively accounts for the behaviour of the spectral function near and below the critical point as well. Note that the other pole moving away from the origin along the imaginary axis as well as the tachyon disappear from G_H at T_c. They remain poles of F only.

In the vicinity of the critical point, where the $\xi = T/8\pi\Phi^2(T)$ is the dominant length scale and the condition $p_0, |\mathbf{p}| << T$ is fulfilled, one can derive an equation also for the soft modes with nonzero momentum:

$$-3i|\mathbf{p}|\xi \frac{p_0^2 - \mathbf{p}^2}{|\mathbf{p}|^2} \ln \frac{p_0 - |\mathbf{p}|}{p_0 + |\mathbf{p}|} - \frac{1}{4\pi} \frac{(p_0^2 - \mathbf{p}^2)\xi}{T_c} \ln \frac{p_0^2 - \mathbf{p}^2}{T_c^2} = 1. \tag{18}$$

Its solution in the approximation, when on the left hand side only the first term is retained exhibits the form of dynamical scaling [14, 15]: $p_0 = |\mathbf{p}|^{\tilde{z}} f(|\mathbf{p}|\xi)$ with $\tilde{z} = 1$. The second term provides the leading correction to scaling. In $O(N)$ models, the dynamical exponent $z = d/2$ has been obtained for finite N on the basis of scaling and renormalisation group arguments, where in our case $d = 3$ [16, 17, 18]. For the correct interpretation of the

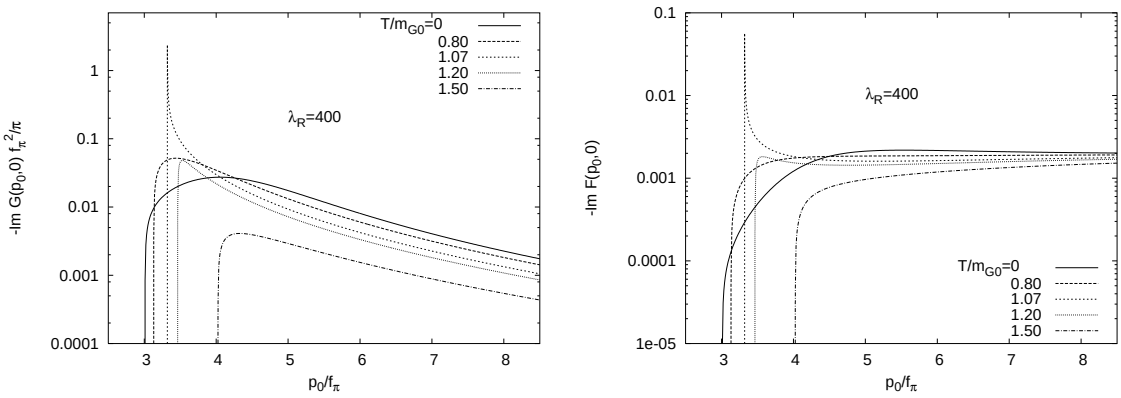

Figure 3: The spectral functions for the linear sigma model with realistic couplings and explicit symmetry breaking. On the left figure the imaginary part in the σ-channel, on the right the same for the composite channel is shown

situation it is important that there are two distinct hydrodynamical regions in the $O(N)$ model for large N [16]. (The system studied in [16] can be regarded as a lattice regularised version of the linear σ-model). In the true critical region $z = d/2$ is valid, in a precritical region $\tilde{z} = 1 - 8S_d/Nd + \mathcal{O}(1/N^2)$, where $S_d = 2/\pi^2$ for $d = 3$. The first region shrinks when N becomes large and completely disappears at $N = \infty$. Furthermore, it has been found that $\tilde{z}$ agrees with the dynamical exponent determined for the quasiparticles, that is outside the hydrodynamical regime, at least to $\mathcal{O}(1/N)$[19]. Details of the application of this analysis to the present case will be published in our forthcoming paper.

4 The case of the explicit breaking of chiral symmetry

Finally, we wish to discuss shortly the results of the application of the leading large N solution of the $O(N)$ model to the low lying effective $\pi - \sigma$ system where an explicit symmetry breaking is necessary.

Since in this case one cannot speak of any phase transition, it is more sensible to look for the roots of $G_H^{-1}(p_0, 0)$ in proportion to $\Phi_0 \equiv f_\pi/2$. The value $m_{G0}^2/\Phi_0^2 \approx 9.06$ is fixed by phenomenology and choosing λ_R with the restriction $M_0/M_L \leq 4$, one can find the zero temperature position of the σ-pole. In Fig.2 its real and imaginary parts are already shown as a function of λ_R together with the results obtained for $h = 0$. In the region of λ_R allowed the ratio M_σ/Γ_σ moves away from the phenomenologically preferred range ($M_\sigma = 3.95 f_\pi, M_\sigma/\Gamma \sim 1.4$) emphasising the need for a next-to-leading order calculation.

Now $\Phi(T)$ is determined from (7). The spectral function of the single σ-channel is shown in the left of Fig.3 for various values of the temperature in the transition range $T = (0 - 1.2)m_{G0}$ with $\lambda_R = 400$. The location of its maximum at $T = 0$ is correlated with the location of the $T = 0$ pole. Maximal threshold enhancement [20] is observed in the close neighbourhood of $1.074 m_{G0}$ with the spectral function numerically exhibiting a cuspy form, with a very narrow width. However, when the temperature is further increased, the maximum is pulled away from the actual position of the threshold and a

broad rounded structure is seen. We return to the detailed interpretation of this structure in terms of the pole trajectories in a forthcoming publication.

As we have mentioned above also the spectral function belonging to the propagator (9) of the composite field can be constructed to leading order in N. The corresponding spectral function reflects the excitations in the composite $(\phi^a)^2$ channel. Its temperature dependent deformation is displayed on the right hand of Fig.3 for the same (realistic) parameters as used in case of ρ_H above. Its behaviour is rather similar to the single meson spectral function. No signal of any meson-meson bound state can be observed. The only difference one notices is that for large frequencies this function approaches a constant, which reflects mostly the large residuum of the tachyon pole in this propagator.

5 Conclusions

We have described the temperature dependence of the elementary excitations of the $O(4)$ model in the leading order of the $1/N$ expansion. For the chirally symmetric case a very suggestive picture of the complex pole evolution makes unique the interpretation of the change of shape of the single-particle spectral function when the temperature approaches the critical point.

The restrictions on the range of the scalar self-coupling λ_R arising from the requirement of keeping distance from the tachyonic pole, for a fixed normalisation point M_0 prevent us in finding a fully realistic σ-particle mass at $T = 0$ when the physical pion mass is the input. We have found that the threshold enhancement in both the elementary and the composite spectral functions is maximal at some $T_{enh} < m_{G0}$. Beyond this temperature the cuspy maximum becomes rounded again. We believe that this qualitative feature remains valid when the next to leading order corrections will be included.

Acknowledgement

This research was supported by the Hungarian Research Fund (OTKA).

References

[1] for a recent review see, T. Hatsuda, Nucl. Phys. **A698** (2002) 243

[2] S. Chiku and T. Hatsuda, Phys. Rev. **58** (1998) 076001

[3] P. Szépfalusy and I. Kondor, Ann. Phys. (N.Y.), **82** (1974) 1, L. Sasvári and P. Szépfalusy, J. Phys. **C7** (1974) 1061

[4] A. Griffin, Excitation in a Bose-Condensed Liquid, Cambridge University Press, Cambridge, 1993

[5] P. Szépfalusy, in *Critical Phenomena*, Lecture Notes in Physics **54**, eds. J. Bray and R.B. Jones, Springer 1976, p.112

[6] F. Cooper, S.Habib, Y. Kluger and E. Mottola, Phys. Rev. **55** (1997) 6471

[7] F. Cooper, S. Habib, Y. Kluger, E. Mottola, J.P. Paz and P.R. Anderson, Phys. Rev. **D50** (1994) 2848

[8] D. Boyanovsky, H.J. de Vega, R. Holman and J. Salgado, Phys. Rev. **D59** (1999) 125009

[9] J. Baacke and K. Heitmann, Phys. Rev. **D62** (2000) 105022

[10] J. Berges, Nucl. Phys. **A699** (2002) 847

[11] G. Aarts, D. Ahrensmeier, R. Baier, J. Berges and J. Serreau, hep-ph/0201308

[12] N.A. Törnquist, hep-ph/0201171

[13] F. Karsch, E. Laermann and A. Peikert, Nucl. Phys. **B605** (2001) 579

[14] R.A. Ferrell, N. Menyhárd, H. Schmidt, F. Schwabl and P. Szépfalusy, Phys. Rev. Lett. **18** (1967) 891, B. I. Halperin and P.C. Hohenberg, Phys. Rev. Lett. **19** (1967) 700

[15] P.C. Hohenberg and B.I. Halperin, Rev. Mod. Phys. **49** (1977) 435

[16] L. Sasvári, F. Schwabl and P. Szépfalusy, Physica **81A** (1975) 108

[17] L. Sasvári and P. Szépfalusy, Physica **87A** (1977) 1

[18] K. Rajagopal and F. Wilczek, Nucl. Phys. **393** (1993)

[19] P. Szépfalusy and L. Sasvári, Acta Phys. Hung. **37** (1974) 343

[20] T. Hatsuda and T. Kunihiro, Phys. Lett. **B185** (1987) 304